

## Use of Strain Gauges to Estimate Pressure in Capillary Rheometers

Carlos Salas-Bringas<sup>1</sup>, Egil Stemsrud<sup>1</sup>, Tom Ringstad<sup>1</sup>, Odd-Ivar Lekang<sup>1</sup>, and Reidar Barfod Schüller<sup>2</sup>

<sup>1</sup> Dep. of Mathematical Sciences and Technology, Norwegian University of Life Sciences, P.O. Box 5003, N-1432 Ås, Norway

<sup>2</sup> Dep. of Chemistry, Biotechnology and Food Science, Norwegian University of Life Sciences, P.O. Box 5003, N-1432 Ås, Norway

### ABSTRACT

The present article describes analytically and experimentally the feasibility of a capillary system that performs indirect pressure measurements in the capillary by strain gauges fixed to the external walls of the capillary.

### INTRODUCTION

In capillary rheometry a large pressure drop is commonly associated with the flow in the die entrance (major) and exit (minor) regions<sup>1, 2</sup>. Today, pressure in capillary rheometers using cylindrical die holes is measured in the reservoir above the capillary die, entrance and exit pressure corrections must be performed to estimate the “true” pressure drop along the capillary die (i.e. Bagley-Rabinowitsch procedure). By measuring the pressure drop ( $\Delta P$ ) between two points in the capillary, it is possible to directly calculate the shear stress at the wall ( $\tau_w$ ) that is a requisite to determine rheological properties. Consequently pressure entry and exit corrections would no longer be required.

The Bagley procedure requires a number of tests that uses different length to diameter ( $L/D$ ) ratios at different shear rates<sup>3</sup>. This results in a large number of experiments that are required to determine the rheological properties of a fluid (e.g.

flow behaviour index ( $n$ ) and consistency index ( $K$ )). Once  $n$  is estimated, the shear rate at the wall ( $\dot{\gamma}$ ) can be calculated.

Sombatsompop and Intawong<sup>4</sup> describe a number of researchers finding such corrections as very difficult to use because: (i) the extension of the imaginary length of the dies ( $N$ ) and pressure values vary with shear rate, (ii) non-linearity of the correction curve, (iii)  $N$  depends on the ratio barrel to die diameter, (iv) negative  $N$  values and (v) the method to determine  $N$  value is experimental, and thus difficult to utilize the process for calculations.

Alternatively to the Weissenberg - Rabinowitsch or Rabinowitsch - Mooney correction<sup>2, 4</sup>, Salas-Bringas et al<sup>5</sup> presented a method that uses less number of dies when different flows are measured, also this method gives the uncertainty of the measurements.

The present article describes an on-going research, presenting the preliminary advances of a development of a measurement principle that directly estimates  $\Delta P$  between two locations at the capillary wall of a rheometer and hence directly estimate  $\tau_w$ . Measurements of pressure are done by strain gauges fixed at the outer surface of the capillary walls which measures the strains produced by pressure.

In addition to the new measuring system, finite element method (FEM) analyses are performed to estimate the strains at the outer walls of the capillary when the capillary holds both, constant pressure and a pressure gradient. This article also shows the results of a calibration procedure using constant pressure.

## MEASUREMENT PRINCIPLE

### Design and development of the capillary die

The capillary die was created in Acrylonitrile butadiene styrene (ABS) using Mojo 3D printer (Stratasys, DDM Group). This allows the creation of complex shapes without the restrictions from milling processes. The capillary has a 3 mm inner diameter and a 0.2 mm thickness in the zones where  $P_1$  and  $P_2$  are located, (see Fig. 1). Externally, not drawn on Fig. 1, a jacket heater connected to a PID controller was assembled to the die to obtain a good temperature control.

Thin walls are preferred in this section to have large enough strains at  $P_1$  and  $P_2$  at low pressure levels.

### Entry angle and elongational flow

The die entry was designed to have a gradual (curved) reduction of the entry angle (clearly seen on Fig. 1). Consequently, a small entry angle is made in the last entry section to facilitate the velocity development of the fluid. Pressure drop should be linear between  $P_1$  and  $P_2$  (see Fig. 1 and Fig. 2).

Mitsoulis and Hatzikiriakos<sup>1</sup> found that excess pressure loss decreases for the same apparent shear rate with increasing contraction angle from  $10^\circ$  to about  $45^\circ$ , and consequently slightly increases from  $45^\circ$  up to contraction angles of  $150^\circ$ . They discovered that shear is the dominant factor controlling the overall pressure drop in flows through small contraction angles. At higher contraction angles ( $> 45^\circ$ ) elongation becomes important<sup>1</sup>. The intent is that excess pressure loss and elongation are

avoided with our die setup. The die entry has contraction angles smaller than  $45^\circ$  from approximately 19 mm above the capillary entry and at 39 mm above the  $P_1$  location (see Fig. 1).

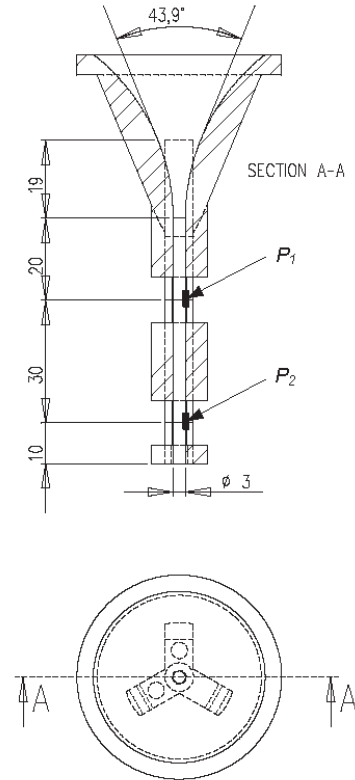


Figure 1. 2D drawing of the die including the location of the strain gauges ( $P_1$  and  $P_2$ ).

The angle of the die entry  $43.9^\circ$  indicates that from 19 mm above the 3 mm diameter capillary, the entry angles are smaller than  $45^\circ$ . Dimensions are in millimetres.

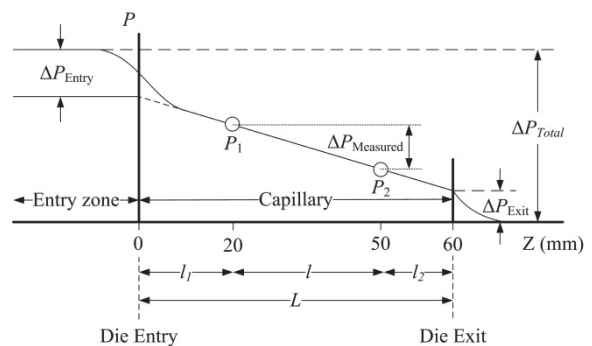


Figure 2. Diagram of pressure distribution in the capillary rheometer (not to scale).

### Installation of the Strain Gauges

The installation of the strain gauges at  $P_1$  and  $P_2$  location was made by HBM, Kolbotn, Norway. The measuring points  $P_1$  and  $P_2$  were cleaned with RMS1 from HBM, then the area was polished with sand paper (220), thereafter the areas were cleaned with RMS1 again. The strain gauges were glued with the rapid adhesive Z70 and a thumb pressure was applied for about one minute at room temperature. The strain gauges were then covered with a protective coating SG 250 (transparent silicone).

One of the installed strain gauges (at  $P_1$ ) is shown on Fig. 3, and the location of both strain gauges can be seen from Fig. 1 and Fig. 2.

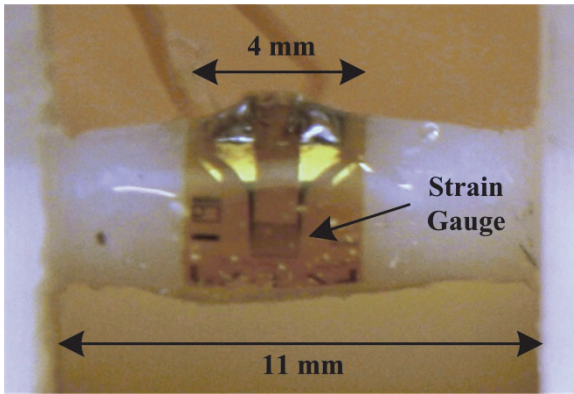


Figure 3. Installed strain gauge at the outer wall of the capillary, picture taken at  $P_1$  location.

### Shear stress from the strain gauges at the capillary wall

Eq. 1 will be used to estimate  $\tau_w$  in the capillary<sup>3</sup>. To apply this equation, the following assumptions must be made: flow is laminar and steady, fluid is incompressible, properties are time and pressure independent, temperature is constant, no slip occurs at the wall of the capillary, radial and tangential velocity components are zero<sup>3</sup> and between  $P_1$  and  $P_2$  the pressure drop should be linear<sup>2</sup>:

$$\tau_w = ((\Delta P_{\text{Measured}}) R) / (2l) \quad (1)$$

where  $\Delta P_{\text{Measured}}$  is the pressure drop between  $P_1$  and  $P_2$ ,  $R$  the capillary radius and  $l$  is the distance between  $P_1$  and  $P_2$ .

### Determination of $n$ value for power law fluids without yield stress

For fluids without yield stress that satisfy the power law model, the following equation can be used<sup>3, 6</sup>:

$$Q = \pi \left( \frac{\Delta P}{2lK} \right)^{1/n} \left( \frac{n}{3n+1} \right) R^{(3n+1)/n} \quad (2)$$

Since  $Q$ ,  $R$ ,  $\Delta P$  and  $l$  are known from this rheometer, it is possible to estimate  $K$  and  $n$  values by solving Eq. 2. To obtain the two unknown variables ( $K$ ,  $n$ ), two equations are needed. The required data can be collected by running the apparatus at a given flow rate ( $Q_1$ ). Eq. 2 can be rearranged as:  $Q_1 - f(R, \Delta P, l, K, n) = 0$  and iteratively find the  $K$  values for a number of  $n$  values. This can be plotted positioning  $n$  in the independent axis and  $K$  on the dependent axis, the result will be a curve. By doing the same procedure for a new  $Q_2$  and plotting the new curve together with the one generated using  $Q_1$ , it will produce an intercept in a point ( $n$ ,  $K$ ) indicating the two unknown values.

Statistical analysis can be performed if more experiments (at different  $Q$ ) are done. The number of crosses or intersections ( $J_N$ ) can be calculated by:

$$J_N = \sum_{i=1}^I i \quad (3)$$

where  $I$  is the number of experiments (or curves) at different  $Q$ . Averages of  $K$  and  $n$  can be estimated with their errors around the mean. This method was presented by Salas-Bringas et al.<sup>2</sup> and later used in Rukke et al.<sup>7</sup> and Salas-Bringas et al.<sup>5</sup>

### Yield stress determination

The yield stress ( $\tau_0$ ) can be determined by a stress relaxation test. This test requires

compressing the material and forcing it to flow through the die. Once this occurs it is possible to stop the piston or RAM, and to record the pressure difference from the measuring points ( $P_1, P_2$  ref. Fig. 2) when a minimum value  $\Delta P_{\min}$  is reached. The yield stress is calculated from a force balance on the fluid as<sup>2, 3</sup>:

$$\tau_0 = \frac{\Delta P_{\min} R}{2l} \quad (4)$$

### Bingham plastic fluids

For these fluids, the Buckingham-Reiner equation for flows in a pipe can be used<sup>3</sup>:

$$\mu_{pl} = \left( \frac{\pi R^4 (\Delta P)}{8 Q l} \right) \left[ 1 - \left( \frac{4}{3} \right) \left( \frac{\tau_0}{\tau_w} \right) + \left( \frac{1}{3} \right) \left( \frac{\tau_0}{\tau_w} \right)^4 \right] \quad (5)$$

where  $\mu_{pl}$  is the plastic viscosity and  $\tau_0$  yield stress. By determining  $Q, R, \Delta P, l, \tau_0$  and  $\tau_w$ , is possible to obtain  $\mu_{pl}$  by performing one experiment at a selected flow rate.

### Herschel-Bulkley fluids

Different equations to estimate the volumetric flow rate of a laminar flow of a Herschel-Bulkley fluid in a circular pipe are given on different literature (Eq. 6<sup>6</sup>, Eq. 7<sup>8</sup> and Eq. 8<sup>3</sup>) where:

$$Q = \pi R^3 n \left( \frac{\tau_w}{K} \right)^{1/n} \left( 1 - \frac{\tau_0}{\tau_w} \right)^{n+1/n} \left[ \frac{\left( 1 - \frac{\tau_0}{\tau_w} \right)^2}{3n+1} + \frac{2 \left( \frac{\tau_0}{\tau_w} \right) \left( 1 - \frac{\tau_0}{\tau_w} \right)}{2n+1} + \frac{\left( \frac{\tau_0}{\tau_w} \right)^2}{n+1} \right] \quad (6)$$

$$Q = \pi R^3 K^{-1/n} \left( \frac{R \Delta P}{2l} \right)^{-3} \left( \frac{R \Delta P}{2l} - \tau_0 \right)^{(n+1)/n} \left[ \left( \frac{R \Delta P}{2l} - \tau_0 \right)^2 \frac{n}{3n+1} + 2 \tau_0 \left( \frac{R \Delta P}{2l} - \tau_0 \right) \frac{n}{2n+1} + \tau_0^2 \frac{n}{n+1} \right] \quad (7)$$

$$Q = \left( \frac{\pi R^3}{256} \right) \left( \frac{4n}{3n+1} \right) \left( \frac{\tau_w}{K} \right)^{1/n} \left( 1 - \frac{\tau_0}{\tau_w} \right)^{1/n} \left[ 1 - \frac{\left( \tau_0 / \tau_w \right)}{2n+1} \left[ 1 + \frac{2n}{n+1} \left( \frac{\tau_0}{\tau_w} \right) \left( 1 + \frac{n \tau_0}{\tau_w} \right) \right] \right] \quad (8)$$

The unknown variables in this system are  $K$  and  $n$ .  $K$  and  $n$  can be determined following the same procedure described to solve Eq. 2. A plot using this method can be found in Rukke et al.<sup>7</sup>

### Diameter of the plug for fluids with yield stress

A plug can be formed in the centre of the capillary when the shear stress  $\tau$  is smaller than the yield stress,  $\tau_0$ .

Determining  $\tau_0$  and  $\tau_w$ , the diameter of the plug ( $D_p$ ) in the centre of the capillary can be easily estimated as follows<sup>6</sup>:

$$D_p = \frac{2 \tau_0 R}{\tau_w} \quad (9)$$

### Stresses and Strain in the capillary

The levels of strain measured by the strain gauges using the set-up shown on Fig. 3 can be easily hand calculated using Eq. 10. Eq. 10 estimates the strain on a circumferential direction on thin cylinders coming from the hoop stresses.

$$\varepsilon_c = \frac{P R}{t E} \left( 1 - \frac{\nu}{2} \right) \quad (10)$$

where  $\varepsilon_c$  is the circumferential strain on thin cylinders having a  $t/R \ll 1/10$ .  $t$  is the thickness of the cylinder and  $R$  is the internal radius.  $E$  is the elastic modulus and  $\nu$  is the Poisson's ratio.

In addition to Eq. 10, FEM analysis using ANSYS 14.5 will be used to estimate the distribution of circumferential strains at the outer face of the capillary wall when an 11 mm long capillary is fully restrained at the ends.

To increase the strength of the entire die section when manually handle, only two capillary sections of 11 mm around  $P_1$  and  $P_2$  were made of thin walls (0.2 mm thickness, see Fig. 3), reason why the FEM analysis will set the capillary ends as fully restrained. The small circumferential strains outside the 11 mm region are consequently neglected.

Beside the calculations using constant pressure at the inner wall of the capillary, it is expected a pressure gradient in the capillary when a fluid flows. Since pressure is not constant under these conditions along the capillary and because the calibration is made using constant pressure, it is of interest to estimate the effect of the neighbouring walls over the strain in the area where the strain gauges are located ( $P_1$  and  $P_2$ ). To investigate this effect, a new FEM analysis is made.

The following data is used to analyse the strain at  $P_1$  and  $P_2$  under constant pressure: capillary length, 11 mm, wall thickness ( $t$ ), 0.2 mm and capillary radius ( $R$ ), 1.5 mm. The mechanical properties of ABS like elastic modulus ( $E$ ), 2250 MPa and the Poisson's ratio, 0,407 are used. A pressure gradient of 5 (MPa/m) with a pressure of 0.2 MPa at  $P_1$  location is used to estimate the effect of the pressure gradient.

The results from Eq. 10 using constant pressure, and the results from FEM analysis using both constant pressure and a pressure gradient, will be plotted together for comparisons (ref. Fig. 5).

### Calibration Procedure

The calibration procedure using constant pressure was initially planned at different temperatures to compensate for the different stiffness's of ABS when working with the die at different temperatures. An inspection of the connection at  $P_1$  location resulted in a breakage of the thin capillary, and consequently only the preliminary results at 30 °C are presented this time.

To obtain the relations between pressure and the signal from the strain gauges, a compression rod was used to press gel trapped between the entry of the capillary die ( $L=0$  according to Fig. 2) and the die exit which was closed. The idea was to form a constant static pressure inside the capillary (from  $L=0$  to  $L=60$ , ref. to Fig. 2). The experiments were repeated three times and six different standard weights attached to the top of the compression rod were used to produce different pressure.

Pressure was calculated using the sum of the mass of the compressing rod made in steel plus the added standard weight. The diameter of the rod in contact with the gel was used to calculate pressure. A gel was selected as a material to fill and transfer pressure during calibration. The viscoelastic nature of the selected gel (ref. to Fig. 7) at 30 °C allows pressure to distribute evenly through the capillary walls. To ensure an evenly distributed gel inside the capillary, the gel was melted at 70 °C and left at this temperature for seven hours to let any possible air bubble escape from the system.

The signals from the strain gauges were set to zero after each test.

### Prediction errors

The equations created from the curve fitting from the experimental results between pressure and raw signal amplitude (see Fig. 8), can be used to create a prediction model to determine pressure from the strain gauge signal. This equation can be used to estimate prediction errors as follows:

$$E \text{ (MPa)} = P_p - A_p \quad (11)$$

where  $P_p$  is the predicted pressure and  $A_p$  the actual pressure.

To obtain an estimation of the most expected errors (in MPa) when using the model to predict new pressure, it was decided to use the root mean square error of prediction ( $RMSEP$ ) that is calculated using

the following equation (Eq. 12) where  $n$  is the number of samples.

$$RMSEP (MPa) = \sqrt{\frac{\sum_{i=1}^n (P_P - A_P)^2}{n}} \quad (12)$$

### PRELIMINARY RESULTS AND DISCUSSIONS

Fig. 4 shows some of the preliminary results to check the sensitivity of the measuring system. This preliminary test was done by HBM, Kolbotn, Norway and it was performed by blowing with the mouth at the die entry. By doing this preliminary test and plotting time (s) versus strain ( $\mu\text{m}/\text{m}$ ), it is possible to estimate the relaxation time of the capillary made in ABS plastic.

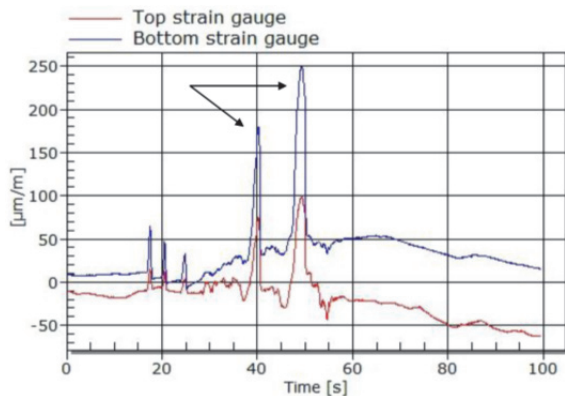


Figure 4. Strains and relaxations in the capillary measured by the strain gauges through an air blowing test. The plot was reported by HBM, Kolbotn, Norway.

The advantage of having a quick relaxation time in capillaries is that this enables performing stress relaxation tests inside the capillary by monitoring the pressure drop over time between the two locations when the rheometer RAM is stopped. The limitation of this system is that the relaxation time of the semi-solid composition should be longer than the relaxation time of the capillary walls.

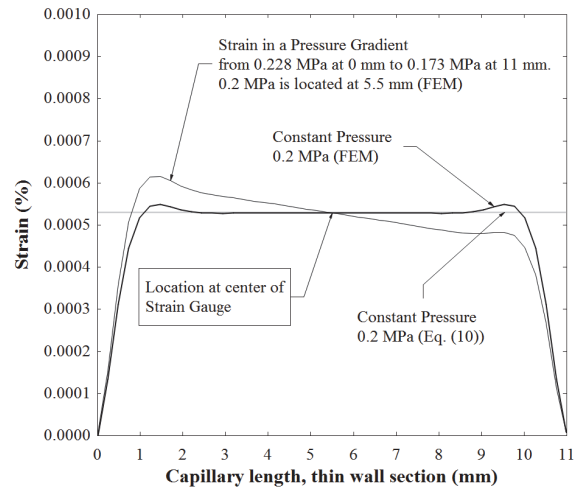


Figure 5. Strain levels using constant pressure given by Eq. 10 and by FEM analysis using both a constant pressure and a pressure gradient when the capillary is fully restrained at the ends (0 and 11 mm).

Fig. 5 shows the calculated values for strain using constant pressure (through Eq. 10 and FEM analysis), and the results using a linear pressure gradient from 0.228 to 0.173 MPa. The values of strain between Eq. 10 and the FEM analysis for 0.2 MPa of constant pressure are the same. Consequently, there is no influence of the thicker walls in the capillary, outside the 11 mm region on the strains at  $P_1$  and  $P_2$ .

The results from Fig. 5 also shows that the same strains occur at the center of the capillary (5.5 mm) if a constant pressure is applied throughout the capillary (calibration procedure), or if a pressure gradient occur through the capillary. Both cases considered a pressure of 0.2 MPa at the centre of the capillary (5.5 mm).

The strains presented on Fig. 6 shows how the thin capillary will expand under a uniform pressure (left side) and under a pressure gradient (right side). As it can be seen on Fig. 6, a similar grey color is located at the middle point (5.5 mm) in both cases.

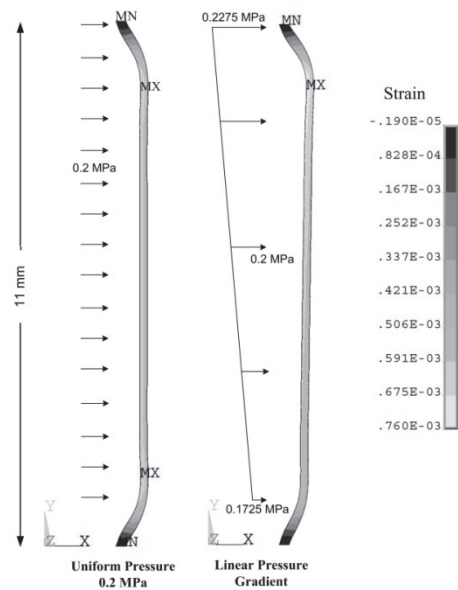


Figure 6. Strains at the capillary walls using FEM analysis, ANSYS 14.5. At the left, strains at the capillary walls using 0.2 MPa of constant pressure. At the right, strains at the capillary walls using a linear pressure gradient along the capillary with a value of 0.2 MPa at the centre to the capillary (strain gauge location). Deformation scale on drawing is 500.

The viscoelasticity of candle gel (Panduro Hobby, Norway) shows that at 30°C, candle gel had  $G' \gg G''$ , its appearance is as a solid gel. This allowed the use of a compression rod having a standard weight on top which was hold by the gel. It is expected that the melted state of the candle gel at 70 °C ( $G'' > G'$ ) allowed a good dispersion of the material inside the capillary for the calibration procedure. As seen on Fig. 7,  $G'$  and  $G''$  remain with similar values after heating or cooling and hence this is a good material when one need to perform calibrations on different dies under similar conditions.

Fig. 8 shows the relations between pressure inside the capillary and the raw signal amplitude given by the two strain gauges. The difference in slope between the curves is possibly due to the installation of the strain gauges is manually made, and it could be that one of them had a thicker layer

of glue or a thicker layer of silicone, or both. The difference in installation between them, however, should not represent any drawback when calibrating the system. The calibration is made using two equations ( $f(\text{pressure, raw signal amplitude})$ ), one for each strain gauge.

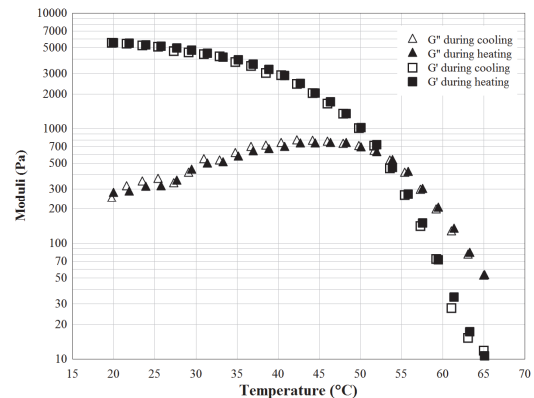


Figure 7. Viscoelasticity of candle gel (Panduro Hobby) during heating and cooling at 10 rad/s and 0.01% strain. Measurements done in a Paar Physica MCR301 rheometer.

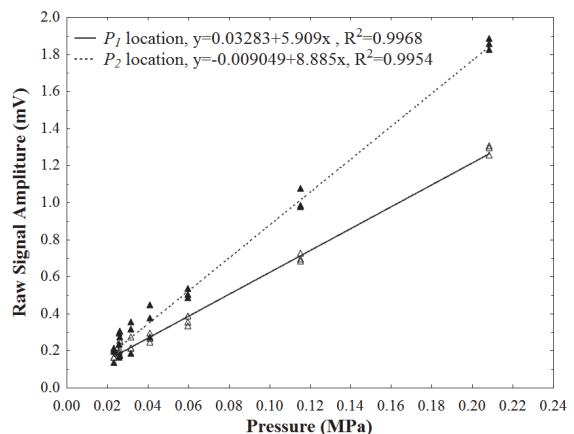


Figure 8. Pressure versus raw signal amplitude (mV) in the strain gauges.  $P_1$  represents the measurements given by the strain gauge at the upstream location and  $P_2$  at the downstream location.

The only inconvenience regarding this calibration method is that it is possible that gel gets trapped between the compressing rod and the inner walls of the capillary, and

this could decrease the amount of pressure that  $P_1$  and  $P_2$  receives. This effect could have caused the dispersion in the data of Fig. 8. The value for RMSEP for the measurements in  $P_1$  is 0.0049 MPa and 0.0062 MPa for  $P_2$ .

It was not possible to continue further with the calibration at this stage (e.g. at different temperatures) as planned because at  $P_1$ , the 0.2 mm capillary wall broke during an inspection to detect the causes of a connection error. Future development should create a new prototype with a more robust connecting system to protect the thin walls. Another alternative is to search for other materials to create a capillary with higher strength, but with low stiffness to obtain enough strains that can be picked up by a strain gauge.

## CONCLUSIONS

An analytical analysis showed that it is feasible to use strain gauges attached to the outer wall of a capillary to obtain the pressure inside the capillary, this allows the possibility to obtain the wall shear stress in the capillary directly, without using pressure corrections as widely done in the present. FEM analysis showed that the existence of a pressure gradient and thus a strain gradient when the fluid flows do not present any disadvantage when predicting pressure inside the capillary. Also, this work shows that a calibration procedure using constant pressure with the signals from the strain gauges can be done. The preliminary data obtained between the pressure inside the capillary and the strains at the outer walls of the capillary showed that this technique is promising. Future work should be done to calibrate the system at different temperatures and possibly to find substitutes for the gel to increase the accuracy of the calibration procedure.

## REFERENCES

1. Mitsoulis, E. and S.G. Hatzikiriakos, (2003), "Bagley correction: the effect of

contraction angle and its prediction", *Rheologica Acta*, **42**: p. 309-320.

2. Salas-Bringas, C., O.-I. Lekang, E.O. Rukke, and R.B. Schüller, (2009), "Development of a new capillary rheometer that uses direct pressure measurements in the capillary", *Annual Transactions of the Nordic Rheology Society*, **17**: p. 39-47.

3. Steffe, J.F., (1996) "Rheological methods in food process engineering". East Lansing, Mich.: Freeman Press. XIII, 418., 0-9632036-1-4

4. Sombatsompop, N. and N.T. Intawong, (2001), "Flow properties and entrance corrections of polymer melts by a mobile barrel capillary rheometer", *Polymer Testing*, **20**(1): p. 97-103.

5. Salas-Bringas, C., O.I. Lekang, and R.B. Schüller, (2010), "Data analysis from capillary rheometry can be enhanced by a method that is an alternative to the Rabinowitsch correction", *Annual Transactions of the Nordic Rheology Society*, **18**: p. 95-100.

6. Chhabra, R.P. and J.F. Richardson, (1999) "Non-Newtonian flow in the process industries". Oxford: Butterworth-Heinemann. xiii, 436 s.

7. Rukke, E.-O., C. Salas-Bringas, O.-I. Lekang, and R.B. Schüller, (2009), "Rheological characterization of liver paste with a new capillary rheometer that uses direct pressure measurements in the capillary", *Annual Transactions of the Nordic Rheology Society*, **17**: p. 243-248.

8. Wildson, C.C., (2001) "Computational Rheology for pipeline and annular flow", 1st edition ed., Woburn, MA: Gulf Professional Publishing. p. 272.